NANO LETTERS

2005
Vol. 5, No. 4
685−691

Continuous Synthesis of Gold Nanoparticles in a Microreactor

J. Wagner*,† and J. M. Köhler†,‡

Physical Chemistry and Microreaction Technology Department, Institute of Physics, Technical University of Ilmenau, Germany, and Institute for Physical High Technology, Jena, Germany

Received January 17, 2005; Revised Manuscript Received February 14, 2005

ABSTRACT

A continuous flow microreactor was used for the synthesis of gold nanoparticles (5 to 50 nm) directly from a gold salt ($HAuCl_4$) and a reducing agent (ascorbic acid). Experimental parameters were optimized to obtain narrow size distributions, which were at average two times narrower than those obtained in a conventional synthesis. Additionally, two approaches, i.e., elevation of pH during reaction and hydrophobization of internal reactor surfaces were tested to suppress reactor fouling.

Over the past decade the research on the synthesis and modification of nanoparticles has had an increasing impact on materials and surface science. Moreover, the discovery of new phenomena, properties, and processes on the nanoscale has led to a wide range of applications and opportunities for nanosized materials. For example, colloidal metal particles show great potential for catalysis[1−4] as well as for analytical applications such as surface enhanced Raman spectroscopy,[5] colorimetric gene detection,[6,7] nanoparticle-enhanced microchip capillary electrophoresis,[8] and optical detection of specific molecular interactions.[9−11] Thus, the synthesis and properties of such particles have attracted considerable scientific and commercial interest, and different classes of substances are under investigation, e.g., organic particles,[12] micellar systems,[13] metal[14] and semiconductor particles,[15−17] oxidic particles,[18,19] as well as complex particles.[20,21]

However, the physical properties of nanoparticles are generally determined by quantum size effects and features such as plasmon band energy of noble metal particles[22,23] and optical band gap of semiconductor particles[16] depend strongly on the particle dimensions, while differing substantially from the bulk material properties. Hence, the control of physical dimensions of such particles, i.e., the control of the particle morphology and the size distribution of the whole sample, is one the most important issues in the synthesis of well-defined nanomaterials. Accordingly the deviation of the mean particle diameter should be as small as possible. Unfortunately most standard syntheses yield particles with rather broad size distributions, and thus microreactors are suggested for these syntheses because simply scaling down the reaction volume was often sufficient to lower the polydispersity of the particle samples.[24] One reason might be efficient and homogeneous mixing in microreactors, which is superior to the heterogeneous flow and mixing conditions in batch reactors.[25] Microreactors provide reaction volumes that are more homogeneous with respect to concentration, temperature, and mass transport, leading to a better control of the reaction steps that govern particle size distribution, i.e., nucleation and growth.[24] Consequently, the obtained particles can be more uniform, although there are difficulties accompanying the handling of heterogeneous systems in microreactors, such as adhesion and transport behavior, which often lead to reactor fouling.

Nevertheless, other groups have worked on this approach as well, and inorganic salt nanocrystallites,[25−29] oxide particles,[30] semiconductor nanoparticles,[31−36] and recently silver particles[37] have been synthesized in a microsystem setup. However, although gold nanoparticles exhibit a range of interesting properties, which have led to a multitude of applications in supramolecular chemistry, molecular biology, catalysis, and nanotechnology (for a review cf. ref 14), to the best of our knowledge no results have been published yet dealing with the direct continuous synthesis of gold nanoparticles in a microsystem. In a previously study we applied a microreactor to investigate the growth of gold nanoparticles from seeds, which were conventionally synthesized outside the microsystem.[38]

In this contribution we report on the extension of this method, to facilitate a simple direct synthesis of gold nanoparticles in a microfluidic setup. In contrast to the earlier

* Corresponding author. FG Physikalische Chemie/Mikroreaktionstechnik, Institut für Physik, TU Ilmenau Weimarer Str. 32, 98693 Ilmenau, Germany, Phone: +49 (0) 3677/69 37 16, Fax: +49 (0) 3677/69 31 79, E-mail: joerg.wagner@tu-ilmenau.de.
† Technical University of Ilmenau.
‡ Institute for Physical High Technology.

10.1021/nl050097t CCC: $30.25
Published on Web 03/16/2005

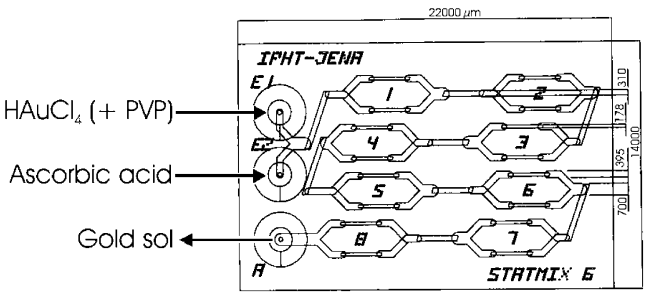

Figure 1. Schematic drawing of the experimental setup showing the connectivity of the IPHT microreactor (STATMIX 6, area 22 × 14 mm).

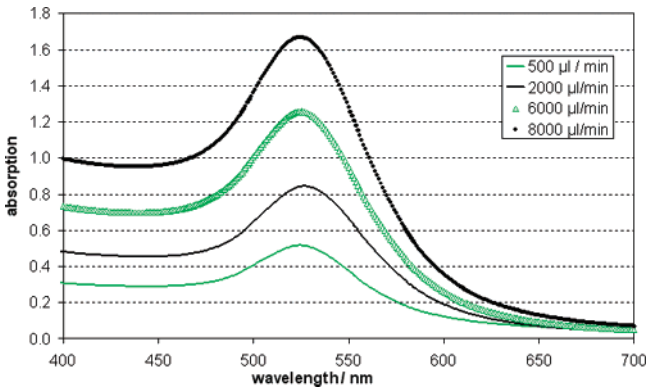

Figure 2. Influence of flow rate: UV−vis spectra of gold colloids showing the degree of nanoparticle adsorption within the reactor at different flow rates (native reactor, pH = 2.8, 1 mM $HAuCl_4$, 20 mM ascorbic acid, 0.025% PVP).

work the educt solutions did not contain any preformed seeds and hence the suppression of gold nucleation at the internal surfaces of the reactor was the main challenge to overcome. Additionally, we screened several experimental parameters and their influence on the produced colloids in this work.

In a typical procedure, chloroauric acid trihydrate and ascorbic acid were dissolved in deionized ultrapure water. The concentration of the chloroauric acid solution was always 1 mM and it contained various amounts of poly(vinylpyrrolidone) (PVP). The concentration of ascorbic acid was 20 mM unless otherwise indicated. If stable pH values were desired during the syntheses the following buffers were used: carbonate buffer pH ∼ 9.7 and phosphate buffer pH ∼7.1. If no buffer was applied, the obtained colloidal solution showed a pH of about 2.8 after leaving the reactor, due to the acidic reaction of excess ascorbic acid. Syringe pumps equipped with polypropylene syringes were used for introducing the educt solutions into the microreactor. The microreactor (IPHT Jena, Germany) is designed as shown in Figure 1, and it was described in detail by Kirner et al. previously.[39] It is a chip-shaped three-layer assembly of wet-etched Pyrex glass and silicon, anodically bonded to each other.

The dimensions of the chip are 22 mm × 14 mm, while the channel width varies between 178 and 700 μm, and the channel depth is 160 μm. The reactor possesses eight split and recombine units (cf. Figure 1), which are designed for an optimal reshaping of the cross-section of stacked fluid column parts. The flow direction is changed from horizontal to vertical and vice versa at branching and reunification points, which facilitates an efficient interdiffusion, i.e., an effective mixing. There are two inlets (E1 and E2) and one outlet (A) while the total interior volume is about 8.5 μL. The reactor was connected to the syringes via flexible PTFE tubing and educt solutions were pumped into the micromixer via inlet E1 and E2 at total flow rates between 500 and 8000 μL/min. Mixing of the two educt streams at ambient temperature was achieved by interdiffusion between the manifold split and recombined lamellae of the laminar stream of both solutions,[39] leading to the generation of colloidal gold particles by reduction of $HAuCl_4$. (Reynolds numbers are between 13 and 200 at these flow rates in this reactor and using the physical properties of water for the calculation.) The produced colloidal solutions left the reactor via outlet A (cf. Figure 1) and were collected in polypropylene centrifuge tubes. After collection, the dispersions were investigated via UV−vis spectroscopy and differential centrifugal sedimentation (DCS). DCS yields directly the particle size distribution of the entire liquid sample. The morphology of the particles was investigated using a scanning electron microscope.

One of the main issues for the synthesis of nanoparticles in microreators is reactor fouling, i.e., the deposition of solid material within the microchannels, that leads eventually to the plugging of the reactor. In this work the microreactors were used only for the production of small volumes of gold nanoparticle dispersion, i.e., less than 10 mL, and not for continuous long-time syntheses. But still, we could observe the deposition of elemental gold or thin violet-colored gold films within the native reactor. To overcome this problem the internal surfaces of the microreactor were chemically modified to reduce reactor fouling, i.e., suppress the deposition of elemental gold within the reactor channels.

The first route to alter the properties of the reactor surfaces was simply to work at an elevated pH (around 9.5), which led to a negative net charge on the silicon surface due to deprotonated Si−OH groups and thus to electrostatic repulsion with the negatively charged gold particles, as described later in detail. Alternatively, the internal surfaces were made hydrophobic via silanization with trichloro(1H,1H,2H,2H-perfluoro-octyl)silane (cf. Supporting Information for details), which reduces the wetting of the channel walls.

In this work we demonstrate the synthesis of gold nanoparticles within a microreactor, which leads to gold particles in the nanometer range (usually between 5 and 50 nm). The half widths of the size distributions were about 35−70% of the mean diameter, which corresponds to a standard deviation (σ) of 15−30% (with respect to the mean diameter). In detail we screened several experimental conditions such as flow rate, pH, concentration ratio, PVP concentration, and the effect of reactor surface modification.

The influence of the flow rate on the plasmon absorption bands of the produced gold sols in the untreated reactor at a pH of ca. 2.8 is shown in Figure 2. The maxima are at 527 nm, corresponding to a deep red color, and one can see that the intensity of the band increases with increasing flow rate.

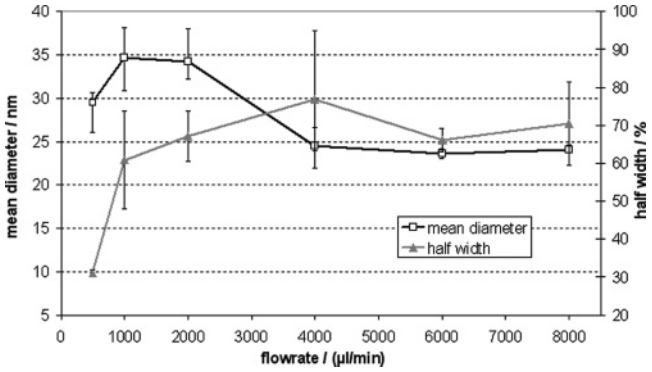

Figure 3. Dependence of size distribution on flow rate (native reactor, pH = 2.8, 1 mM $HAuCl_4$, 20 mM ascorbic acid, 0.025% PVP).

Hence, it is assumed that the adsorption of nanoparticles or nanoparticle nuclei on the inner surfaces of the reactor is a function of the flow rate. Presumably at rather low flow rates the reduction of gold ions to elemental gold takes place at the walls of the reactor channels preferentially, where the surface itself serves as nucleation starter. Surface-bound reduction on the inner walls is indicated by the formation of thin films of elemental gold on the inner channel walls, which is recognizable by a violet color, which is observable at the points where the reactor is transparent. In the course of the synthesis the film becomes darker and eventually opaque, indicating either the growth of the film thickness or the incorporation of gold particles or particle aggregates into the film. One can conclude that working with rather high flow rates minimizes the possibility of surface interactions due to higher surface sheer energy. That in turn leads to less reactor fouling, i.e., deposition of elemental gold on the channel surfaces. In this way one can obtain higher concentrated gold sols, which corresponds to higher particle yields.

In contrast to the concentration, the size distribution of the dispersion is less affected by the flow rate (Figure 3). The mean particle diameters are between 24 nm at 8000 μL/min and 35 nm at 100 μL/min, and only a slight trend to smaller mean diameters at higher flow rates is observable. The largest mean diameter is approximately 35 nm and it goes down to 24 nm, presumably due to higher nucleation rates at higher flow rates. The higher the flow rates, the shorter the retention time is in the reactor (hydrodynamic retention time: 1.02 s at 500 μL/min and 0.06 s at 8000 μL/min). This results in faster multilamination and thus in greater gradients between the lamellae and smaller interdiffusion times between the lamellae. Eventually this leads to faster and more efficient mixing of the lamellae, resulting in a quick propagation of excess reducing agent into the Au^+-containing lamella. Accordingly, the nucleation is the favored process (greater nucleation rates than growth rates) and nuclei growth is somewhat repressed. This, however, leads to a higher number of smaller particles, since more particles are formed and particle growth is restricted by the total amount of gold available.[40] In other words, higher flow rates seem to support a shorter nucleation phase compared to the growth time, which is favorable for a narrow size distribution.[24] The half width of all distributions is around 70% of the mean

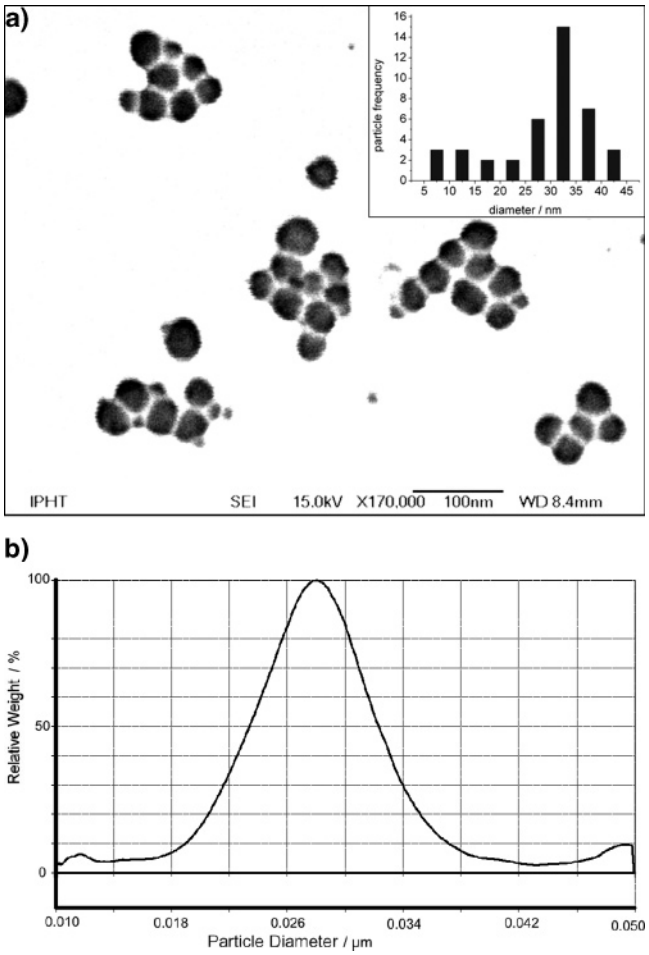

Figure 4. (a) SEM image (with particle size analysis as inset) of gold particles obtained at a flow rate of 500 μL/min (native reactor, pH = 2.8, 1 mM $HAuCl_4$, 20 mM ascorbic acid, 0.025% PVP). (b) DCS spectrum of the same sample.

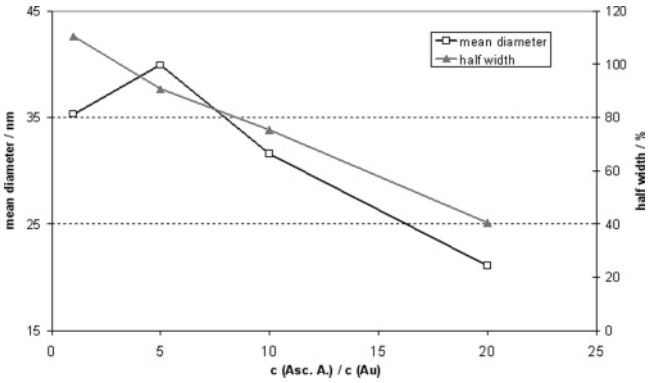

Figure 5. Dependence of size distribution on concentration ratio (native reactor, pH = 2.8, 1 mM $HAuCl_4$, varying ascorbic acid concentrations, 0.025% PVP, total flow 2000 μL/min).

diameter, which corresponds to a σ of approximately 30% of the mean diameter. Solely at a total flow of 500 μL/min the half width of the size distribution is considerably lower: 31% (corresponding to σ = 13%) compared to all other flow rates (Figure 4), a result we cannot explain conclusively, yet.

Figure 5 shows the correlation between concentration ratio (reducing agent/gold ions) and the resulting size distribution. It shows that an increasing concentration of the reducing

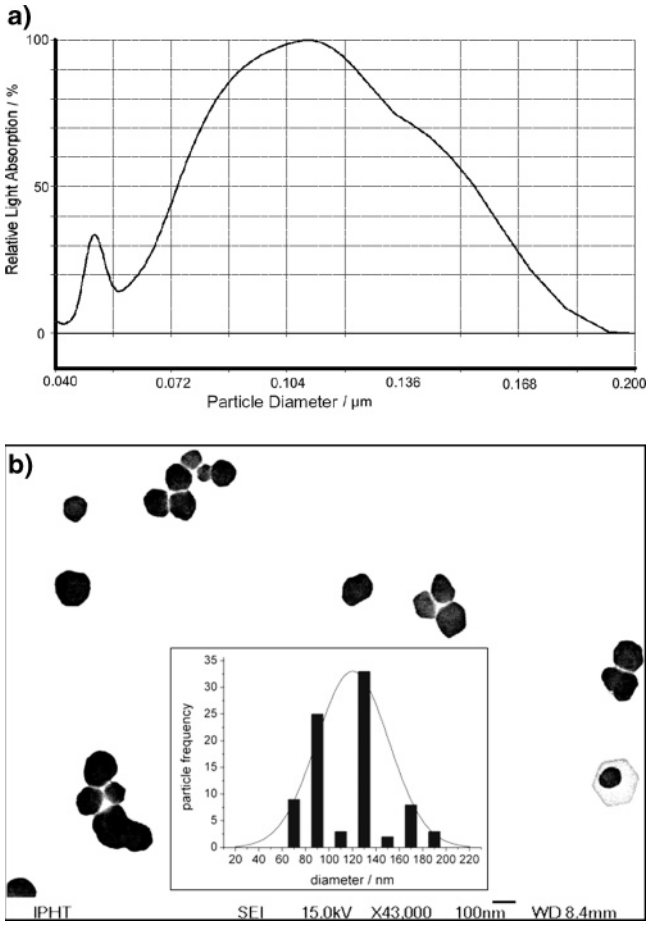

Figure 6. (a) DCS spectra and (b) SEM image of gold nanoparticles obtained at a concentration ratio c ($HAuCl_4$)/c (ascorbic acid) = 1 (native reactor, pH = 2.8, 1 mM $HAuCl_4$, 1 mM ascorbic acid, 0.025% PVP, total flow 2000 μL/min). Inset: particle statistics obtained from a lower magnified SEM image of the same sample.

agent (ascorbic acid) leads to a decrease of the mean diameter and of the half width as well. At a 1:1 ratio of ascorbic acid to gold we observed a different size distribution in each produced sample, suggesting very unstable reduction conditions at this ratio. In fact, we observed at this concentration ratio mean diameters with a standard deviation of 75% within the three analyzed samples, while at all other concentration ratios the deviation within the samples was below 11%.

The DCS analysis of one of these 1:1 samples showed a very broad size distribution with a mean diameter of approximately 110 nm (Figure 6a, the peak at ca. 50 nm is assigned to an impurity). The SEM image of this sample (Figure 6b) supports the DCS measurement and shows some larger particles (bigger than 150 nm) as well as some smaller ones, while the mean diameter is ca. 115 nm. When an excess of ascorbic acid was applied, the quality of the obtained gold particles improved and, at a ratio of 20:1, dispersion with a mean gold particle diameter of 21 nm was obtained, where the half width of the distribution was only 8.5 nm (~40%) or $\sigma = 3.6$ nm (~17%). This trend is clearly due to the higher number of nuclei formed at the start of the reaction since the reducing agent is present in a high concentration. The subsequent growth period is rather short since there are many nuclei that grow, and the reaction is quenched as soon as all

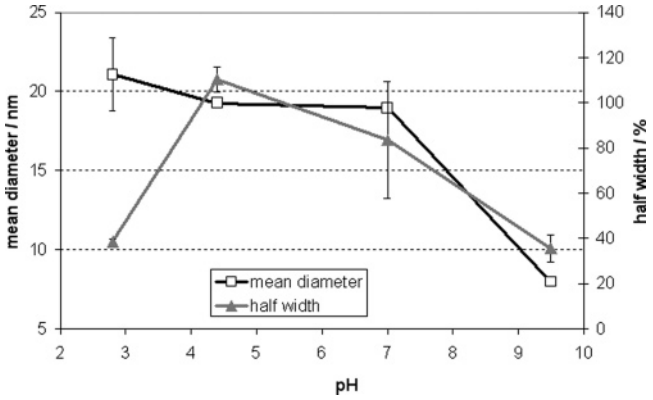

Figure 7. Influence of pH on the size distribution (native reactor, 1 mM $HAuCl_4$, 20 mM ascorbic acid, 0.0025% PVP, total flow 2000 μL/min).

gold is used, while the rather weak capping agent ascorbic acid does not inhibit the growth as much as, for example, thiols do.[41] Consequently, at high reducing agent-to-gold ratios, usually small particles with a narrow size distribution are formed, a process that can be assisted even more by stronger capping agents.[41]

As one can expect, the mean diameter decreases with increasing pH (Figure 7): 21 nm at pH = 2.8 to 8.0 nm at pH = 9.5. Moreover, the half width is reduced from 54% at pH = 2.8 to 36% at pH = 9.5. These findings are a consequence of choosing ascorbic acid as the reducing agent. The redox potential of ascorbic acid is a function of the pH, according to Nernst's equation: The higher the pH, the more negative the redox potential of ascorbic acid is and the stronger its reducing power is. Accordingly, more nuclei are formed at greater rates, leading to a reduced growth time and, thus, to a narrower distribution with a smaller mean diameter. Furthermore, a higher pH of the reaction medium can also repress particle adsorption on the surface, due to electrostatic effects. The surface of native silicon and glass, of which the reactor is made, is hydrophilic. It consists of SiO_2 and Si−OH groups,[42] whose density is considered to be 5×10^{14} OH-groups/cm^2.[43] Depending on the pH value of the fluid inside the reactor and the pK_a of the surface OH groups (between 4 and 9),[44] these groups can also occur as deprotonated Si−O^- groups. This property can be utilized to deprotonate the surface Si−OH groups, which leads to negative net charge on the surface. Provided the ascorbate-stabilized particles have a negative charge on their surface (which they should have at a pH of 9.5, since pK_{a2} = 11.5 for ascorbic acid), the particles repel from the reactor surface due to electrostatic interaction.

To study the effect of the polymer additive PVP, the pH was adjusted to 9.5 to facilitate the formation of preferably small particles with a narrow size distribution and the concentration of PVP was varied. PVP is a water soluble uncharged polymer that is used for steric stabilization of colloids.[45] Figure 8 shows how the size distribution of the produced gold sol is affected by an increased concentration of PVP. Higher contents of PVP up to 0.125% lead to a slight reduction in the mean particle diameter, while at higher concentrations (above 0.15%) no further decrease was

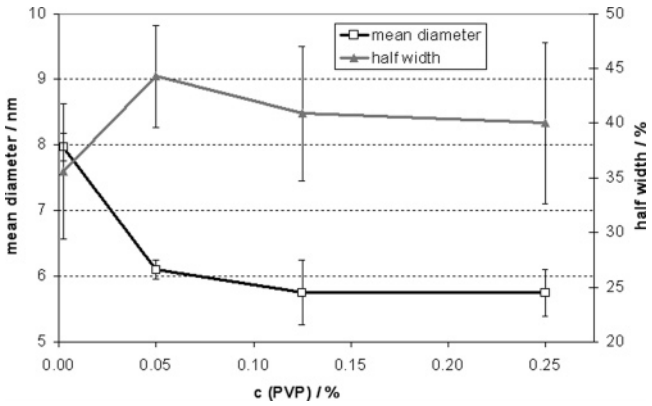

Figure 8. Effect of PVP concentration on the particle size distribution (native reactor, pH = 2.8, 1 mM $HAuCl_4$, 20 mM ascorbic acid, 0.025% PVP, total flow 2000 μL/min).

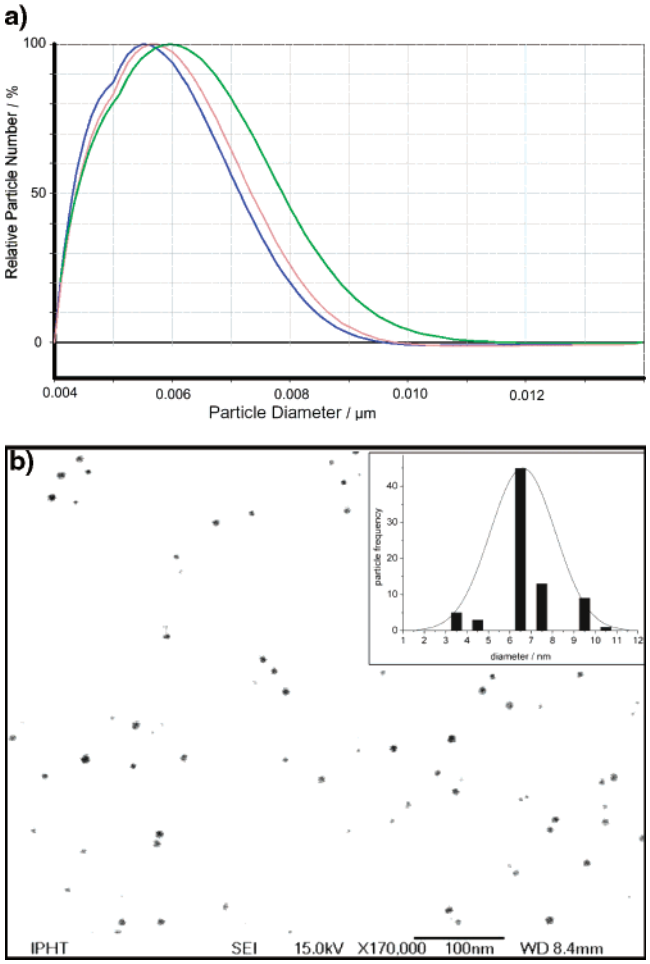

Figure 9. (a) DCS of three samples of 6 nm gold particles obtained at a c(PVP) = 0.25%, (native reactor, pH = 9.5, 1 mM $HAuCl_4$, 20 mM ascorbic acid, total flow 2000 μL/min) and (b) SEM image of one of these samples; inset: particle statistic of this image.

observed. This finding could also be a result of the poor resolution of the DCS system. It is limited by diffusion, and thus particles smaller than 6 nm in diameter are at the size detection limit of the system, thus they are hardly observed reliably and lead to very asymmetric peaks (Figure 9a). An explanation for the significant decrease in particle size with increasing PVP content could be as follows: The probably random coiled polymer chains slow the diffusion of gold ions within the solutions, especially in the neighborhood of nuclei bearing PVP molecules. This supports the formation of more nuclei because the growth is restricted since the gold ions cannot move fast enough to the gold depleted region around a just-formed nuclei. In sum, this leads to higher nucleation rates immediately after reaching the nucleation concentration, where growth and further nucleation are competing processes.[24] Less information can be drawn about the half width of the distribution since it shows rather large standard deviation, which is probably due to the applied DCS technique. As mentioned before, at very small particle diameters, <6 nm, the sedimentation within the DCS centrifuge lasts longer (up to 30 min), even at high gravitational forces, and the width of the distribution is therefore governed by diffusion within the system during analysis (i.e., Brownian motion) rather than by the original width of the particle size distribution.

However, the SEM image in Figure 9b shows particles obtained at a PVP concentration of 0.25%, and a measurement of 109 of these particles in the image revealed a mean diameter of 5.6 nm (cf. inset in Figure 9b), a value that is in good accordance with the DCS measurement, where we found a mean diameter of 5.3 nm (cf. Figure 9a). Another source of error could be the adsorption of PVP on the gold particle surfaces. If the PVP substitutes ascorbate ions on the surface (at least partially), the polymer chains will have a much greater influence on the physical properties of the particles compared to ascorbate ions, because of their high molecular weight. The mean density of these particles will change, and even more importantly the (bulky) polymer chains on the surface will lower the sedimentation velocity of the particles during DCS analysis. This in turn will lead to measured diameters smaller than the real ones.

To compare the size distributions obtained in the microreactor with those obtained applying conventional synthesis equipment, we set up a series of reference experiments using a 25 mL beaker and a 15 mL flask. The syntheses in these containers were performed at pH = 2.8 and also at pH = 9.5. The experiments in the flask were also repeated twice to ensure reproducibility. The DCS analysis of the gold particles obtained in the beaker at pH = 2.8 shows two peaks at approximately 49 and 91 nm with a half width of about 37 nm (75 and 42%, respectively) for both peaks (Supporting Information). At pH = 9.5 the distribution is monomodal with a mean diameter of 31 nm and a half width of about 20 nm (64%) and σ = 27% displaying a higher nucleation rate due to the higher pH, as explained before. The syntheses carried out in the flask were executed twice at each pH and are shown. At pH = 2.8 the particles are rather big with a mean diameter of about 47 nm (mean of both syntheses) and a mean half width of 41 nm (86%), corresponding to σ = 17 nm (37%). Contrarily, at pH = 9.5 small particles with a mean diameter of 11.2 nm and a half width of 7.5 nm (66.5%), corresponding to σ = 3.2 nm (28%) were obtained. However, it becomes clear that the particle size distributions achieved with the conventional equipment are of lower

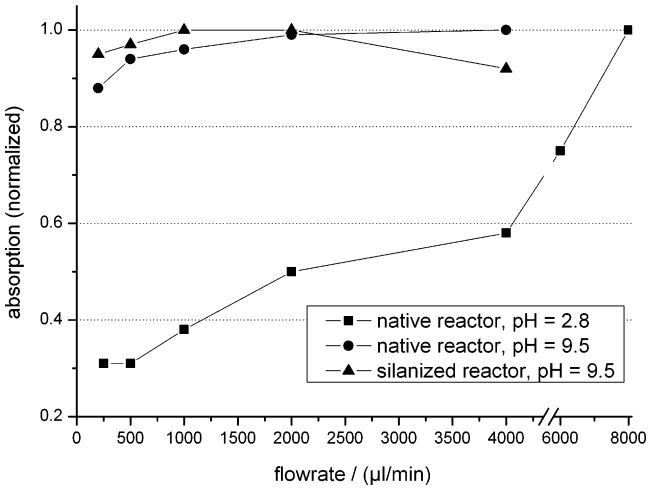

Figure 10. Observed maximum absorptions of colloidal solutions (normalized with the highest absorption value observed for each reaction regime) synthesized in different pretreated reactors and at various pH values (1 mM $HAuCl_4$, 20 mM ascorbic acid, 0.025% PVP).

quality compared to the ones obtained in the microreactor at the same conditions.

Optimized syntheses in the microreactor at H = 2.8 with 500 μL/min and at a 20:1 gold-to-ascorbic acid ratio yielded size distributions with $\sigma = 13\%$ and $\sigma = 17\%$, respectively. These distributions are by a factor of 2 smaller than those obtained in the flask or beaker. At pH = 9.5 the best distributions obtained in the microreactor show $\sigma = 15\%$, and they are rarely broader than $\sigma = 20\%$, which is also two times smaller than the width of the size distributions obtained with the conventional lab equipment.

Comparison of the correlation between flow rate and the (normalized) UV−vis absorption at the plasmon peak maximum (Figure 10), which is a measure for the particle yield, leads to the following conclusions. In the native silicon/glass reactor operated at basic conditions, the obtained concentration of gold particles becomes almost independent from the flow rate, as shown by the slight increase of the absorption when we worked at higher flow rates. At a total flow of 200 μL/min we observed 88% of the maximum absorption, which was detected at 4000 μL/min (the flow rate was not increased further). The reason is the opposite charge of particles and channel surfaces, which suppresses the interaction between them. Similarly, we observed only a very weak correlation between flow rate and observed absorption value when we investigated the absorption of the gold sols produced in the silanized reactor, where the effect is due to the hydrophobic surface of the reactor. Here, the particle yield shows a slight increase from 92% at 200 μL/min to the maximum, which was detected at a flow rate of 1000 μL/min and also at 2000 μL/min. It decreased a little when we worked at 4000 μL/min, where we observed 95% of the maximum absorption. But these small deviations ($\leq$8%) could also be within the experimental variation of the concentration and age of the reactant solutions and, in our opinion, do not correspond to real effects. However, a distinct positive correlation between flow rate and particle yield was observed in the native reactor at pH = 2.8, as one can see in Figure 10, where the normalized absorption increases from 31% at 250 μL/min to its maximum at 8000 μL/min. It is even possible to fit these data to a linear function with a correlation coefficient of $R^2 = 0.98$ and a slope of approximately 0.08/1000 (μL/min). Clearly, this is due to the high degree of interaction between the particles (and particle seeds) with the channel walls. Accordingly, this effect is suppressed by employing higher sheer forces, i.e., enhancing the flow rate, since sheer forces are linearly dependent on the flow rate at laminar flow conditions.

In summary, gold nanoparticles were synthesized in a glass−silicon microreactor at continuous flow conditions. The mean diameter and the width of the particle size distribution were adjusted by tuning experimental parameters such as flow rate, pH, excess of reducing agent, and concentration of PVP. Particles with mean diameters between 5 and 50 nm were obtained, and the best size distribution possesses a standard deviation (σ) of about 13%, that is two times smaller than the mean σ we achieved in syntheses conducted using conventional lab equipment.

An important issue was the surface treatment of the inner walls of the microreactor, since adhesion of gold particles or their nuclei to these surfaces was a major drawback. However, we were able to reduce this problem via two alternative approaches. One was the silanization of the reactor, which led to hydrophobic surfaces and hence less wetting of these surfaces, resulting in an independence of particle yield from flow rate and leading to no reactor fouling. On the other hand, we worked at an elevated pH, which reduced the deposition due to a net negative charge on the particles and the reactors internal surface, leading to mutual repulsion.

Acknowledgment. We thank the cleanroom staff and especially J. Albert at the Institute of Physical High Technology (IPHT) Jena for the production of the micrormixer. For the SEM measurements we are grateful to A. Assmann at IPHT Jena. Furthermore, we thank F. Möller (TU Ilmenau) for assistance with the experiments and C. v. Teichmann (TU Ilmenau) for her suppport in the preparation of this manuscript. This work was funded by German Federal Environmental Foundation (DBU).

Supporting Information Available: Experimental details and DSC analyses of the samples prepared in the beaker and flask, respectively. This material is available free of charge via the Internet at http://pubs.acs.org.

References

(1) Mingotaud, A. F.; Reculusa, S.; Mingotaud, C.; Keller, P.; Sykes, C.; Duguet, E.; Ravaine, S. *J. Mater. Chem.* **2003**, *13*(8), 1920−1925.
(2) Marcial Moreno-Manas, M.; Pleixats, R. *Acc. Chem. Res.* **2003**, *36*, 638−643.
(3) Mukherjee, P.; Patra, C. R.; Ghosh, A.; Kumar, R.; Sastry, M. *Chem. Mater.* **2002**, *14*(4), 1678−1684.
(4) Crooks, R. M.; Zhao, M. Q.; Sun, L.; Chechik, V.; Yeung, L. K. *Acc. Chem. Res.* **2001**, *34*(3), 181−190.
(5) Shipway, A. N.; Katz, E.; Willner, I. *ChemPhysChem* **2000**, *1*(1), 18−52.
(6) Köhler, J. M.; Csaki, A.; Reichert, J.; Moller, R.; Straube, W.; Fritzsche, W. *Sens. Actuators, B* **2001**, *76*(1−3), 166−172.

(7) Fritzsche, W.; Taton, T. A. *Nanotechnology* **2003**, *14*(12), R63−R73.
(8) Pumera, M.; Wang, J.; Grushka, E.; Polsky, R. *Anal. Chem.* **2001**, *73*(22), 5625−5628.
(9) Henglein, A. *Chem. Mater.* **1998**, *10*, 444−450.
(10) Nath, N.; Chilkoti, A. *Anal. Chem.* **2002**, *74*(3), 504−509.
(11) Kim, Y.; Johnson, R. C.; Hupp, J. T. *Nano Lett.* **2001**, *1*(4), 165−167.
(12) Marguerettaz, X.; Merrins, A.; Fitzmaurice, D. *J. Mater. Chem.* **1998**, *8*(10), 2157−2164.
(13) Pileni, M. P. *Langmuir* **1997**, *13*, 3266−3276.
(14) Daniel, M. C.; Astruc, D. *Chem. Rev.* **2004**, *104*(1), 293−346.
(15) Bley, R. A.; Kauzlarich, S. M. In *Nanoparticles and nanostructured films*; Fendler, J. H., Ed.; Wiley VCH: New York, 1998; p 101.
(16) Alivisatos, A. P. *J. Phys. Chem.* **1996**, *100*, 13226−13239.
(17) Parak, W. J.; Gerion, D.; Pellegrino, T.; Zanchet, D.; Micheel, C.; Williams, S. C.; Boudreau, R.; Le Gros, M. A.; Larabell, C. A.; Alivisatos, A. P. *Nanotechnology* **2003**, *14*(7), R15−R27.
(18) Allen, M.; Willits, D.; Young, M.; Douglas, T. *Inorg. Chem.* **2003**, *42*(20), 6300−6305.
(19) McCormick, P. G.; Tsuzuki, T. *Metastable, Mech. Alloyed Nanocryst. Mater.* **2002**, *386*(3), 377−386.
(20) Hernandez-Padron, G.; Rojas, F.; Castano, V. N. *Nanotechnology* **2004**, *15*(1), 98−103.
(21) Hiramatsu, H.; Osterloh, F. E. *Langmuir* **2003**, *19*(17), 7003−7011.
(22) Link, S.; El-Sayed, M. A. *J. Phys. Chem. B* **1999**, *103*, 4212−4217.
(23) Schmid, G.; Chi, L. F. *Adv. Mater.* **1998**, *10*(7), 515−526.
(24) DeMello, J.; DeMello, A. *Lab On A Chip* **2004**, *4*(2), 11N-15N.
(25) Schenk, R.; Hessel, V.; Jongen, N.; Buscaglia, V.; Guillement-Fritsch, S.; Jones, A. G. *Encyclopedia of Nanoscience and Nanotechnology* **2004**, *7*, 287−296.
(26) Jongen, N.; Donnet, M.; Bowen, P.; Lemaitre, J.; Hofmann, Ch.; Schenk, R.; Hofmann, H.; Aoun-Habbache, M.; Guillement-Fritsch, S.; Sarrias, J.; Rousset, A.; Viviani, M.; Buscaglia, M. T.; Buscaglia, V.; Nanni, P.; Testino, A.; Herguijuela, J. R. *Chem. Eng. Trans.* **2002**, *1*, 807−812.
(27) Jongen, N.; Donnet, M.; Bowen, P.; Lemaitre, J.; Hofmann, H.; Schenk, R.; Hofmann, C.; Aoun-Habbache, M.; Guillemet-Fritsch, S.; Sarrias, J.; Rousset, A.; Viviani, M.; Buscaglia, M. T.; Buscaglia, V.; Nanni, P.; Testino, A.; Herguijuela, J. R. *Chem. Eng. Technol.* **2003**, *26*(3), 303−305.
(28) Schenk, R.; Donnet, M.; Hessel, V.; Hofmann, Ch.; Jongen, N.; Löwe, H. *Proc. 5th Int. Conf. Microreation Technol.* **2001**, 489−498.
(29) Schenk, R.; Hessel, V.; Werner, B.; Schönfeld, F.; Hofmann, Ch.; Donnet, M.; Jongen, N. *Chem. Eng. Trans.* **2002**, *1*, 909−914.
(30) Wang, H. Z.; Nakamura, H.; Uehara, M.; Miyazaki, M.; Maeda, H. *Chem. Commun.* **2002**, (14), 1462−1463.
(31) Nakamura, H.; Tashiro, A.; Yamaguchi, Y.; Miyazaki, M.; Watari, T.; Shimizu, H.; Maeda, H. *Lab On A Chip* **2004**, *4*(3), 237−240.
(32) Wang, H. Z.; Li, X. Y.; Uehara, M.; Yamaguchi, Y.; Nakamura, H.; Miyazaki, M. P.; Shimizu, H.; Maeda, H. *Chem. Commun.* **2004**, (1), 48−49.
(33) Chan, E. M.; Mathies, R. A.; Alivisatos, A. P. *Nano Lett.* **2003**, *3*(2), 199−201.
(34) Nakamura, H.; Yamaguchi, Y.; Miyazaki, M.; Uehara, M.; Maeda, H.; Mulvaney, P. *Chem. Lett.* **2002**, *31* (10), 1072−1073.
(35) Nakamura, H.; Yamaguchi, Y.; Miyazaki, M.; Maeda, H.; Uehara, M.; Mulvaney, P. *Chem. Commun.* **2002**, (23), 2844−2845.
(36) Edel, J. B.; Fortt, R.; deMello, J. C.; deMello, A. J. *Chem. Commun.* **2002**, (10), 1136−1137.
(37) Lin, X. Z.; Terepka, A. D.; Yang, H. *Nano Lett.* **2004**, *4*(11), 2227−2232.
(38) Wagner, J.; Kirner, T.; Mayer, G.; Albert, J.; Köhler, J. M. *Chem. Eng. J.* **2004**, *101*(1−3), 251−260.
(39) Kirner, T.; Albert, J.; Gunther, M.; Mayer, G.; Reinhackel, K.; Köhler, J. M. *Chem. Eng. J.* **2004**, *101*(1−3), 65−74.
(40) Turkevich, J.; Stevenson, P. C.; Hillier, J. *Discuss. Faraday Soc.* **1951**, *11*, 55−75.
(41) Jana, N. R.; Gearheart, L.; Murphy, C. J. *Langmuir* **2001**, *17*(22), 6782−6786.
(42) Wasserman, S. R.; Tao, Y.-T.; Whitesides, G. M. *Langmuir* **1989**, *5*, 1074−1087.
(43) Brunner, H.; Basnar, B.; Friedbacher, G.; Hoffmann, H.; Vallant, T.; Mayer, U. *Langmuir* **1999**, *15*(6), 1899−1901.
(44) Kopelman, R.; Zhao, X. *J. Phys. Chem.* **1996**, *100*, 11014−11018.
(45) Han, M. Y.; Quek, C. H.; Huang, W.; Chew, C. H.; Gan, L. M. *Chem. Mater.* **1999**, *11*, 1144−1147.

NL050097T